

1 **Dynamics of the impact of ENSO flavors on precipitation**
2 **over La Plata Basin***

3 Laura Zamboni^{1,2}, Annalisa Cherchi^{1,3}, Marcelo Barreiro⁴, and Fred Kurcharski⁵

4 ¹Centro Euro-Mediterraneo per i Cambiamenti Climatici, Italy

5 ²Mathematics and Computer Science Division, Argonne National Laboratory, Argonne,
6 IL, USA

7 ³Istituto Nazionale di Geofisica e Vulcanologia, Italy

8 ⁴Facultad de Ciencias, Universidad de la Republica, Uruguay

9 ⁵Abdus Salam International Centre for Theoretical Physics, Earth System Physics
10 Section, Italy

11 Manuscript submitted to

12 **Climate Dynamics**

13 February 17, 2012

14 **Corresponding author:**

15 Laura Zamboni

16 Mathematics and Computer Science Division

17 Argonne National Laboratory

18 Argonne, IL (USA)

19 E-mail: lzamboni@mcs.anl.gov

*The submitted manuscript has been created by UChicago Argonne, LLC, Operator of Argonne National Laboratory (Argonne). Argonne, a U.S. Department of Energy Office of Science laboratory, is operated under Contract No. DE-AC02-06CH11357. The U.S. Government retains for itself, and others acting on its behalf, a paid-up nonexclusive, irrevocable worldwide license in said article to reproduce, prepare derivative works, distribute copies to the public, and perform publicly and display publicly, by or on behalf of the Government.

Abstract

In this study we use observational datasets and two atmospheric general circulation models to demonstrate that the mechanism linking the canonical El Niño Southern Oscillation (ENSO) to precipitation anomalies in La Plata Basin (LPB) during the austral Spring is found even when Sea Surface Temperature anomalies (SSTa) are largest over the central Pacific (Dateline El Niño). Corresponding to both flavors, increased (decreased) precipitation is observed during El Niño (La Niña) in LPB, while opposite anomalies occur to the northeast of South America (SA). In contrast, positive loads shift to the north when SSTa are uniform from the eastern to the central Pacific in what forms the additional flavor (Spread) we document here.

Besides the dynamical features already reported in the literature for the impact of ENSO in LPB, we found evidence of an additional wave train emanated from the tropical Pacific meridionally toward the southern hemisphere in our modeling experiments. This wave can be a standalone pattern but also interfere and amplify the Pacific-South American Mode over the eastern Pacific and SA. Additionally, we provide evidence of a Gill type of response to the east of the heating region and whose effects are appreciated on the local circulation over SA and thus precipitation over LPB.

39 **1 Introduction**

40 A number of studies have recently suggested the existence of an El Niño-like phenomenon dif-
41 ferent from that previously described for the "canonical" ENSO; among its main characteristics is
42 the presence of largest Sea Surface Temperature anomalies (SSTa) over the central Pacific rather
43 than closer to the South American coast. The new El Niño has been referred to as Dateline (Larkin
44 and Harrison 2005a), Central Pacific (Kao and Yu 2009), Warm Pool (Kug et al. 2009), Modoki
45 (Ashok et al. 2007), and Summer type (Xu and Chan 2001) El Niño. Trenberth and Stepaniak
46 (2001) named the new and canonical types collectively as different "flavors" of El Niño.

47 A natural question is whether different impacts can be expected when different flavors occur.
48 Sensitivities have already been reported globally (Larkin and Harrison 2005a, Ashok et al. 2007)
49 as well as regionally for the USA (Larkin and Harrison 2005b, Mo 2010), Australia (Wang and
50 Hendon 2007), the countries in the Pacific rim (Weng et al. 2007), and China (Feng and Li 2011).

51 In the present paper, we explore the impact of different flavors of the El Niño Southern Oscilla-
52 tion (ENSO) on precipitation over La Plata Basin (LPB). The region, comprising southern Brazil,
53 Uruguay, northeastern Argentina, southern Paraguay, and southern Bolivia, is particularly affected
54 by the variability associated with ENSO (e.g., Aceituno 1988, Rao and Hada 1990, Grimm et
55 al. 1998, Montecinos et al. 2000), since it strongly relies on agriculture and hydroelectricity
56 production. The positive phase of ENSO (El Niño) tends to generate increased seasonal precip-
57 itation over LPB and drier conditions over northeast South America (SA) both associated with
58 anomalous intensity and direction of the South American Low-Level Jet (SALLJ) (Ferreira et al.
59 2003, Liebmann et al. 2004, Silva et al. 2009). The sign of anomalies reverses during La Niña
60 (Grimm et al. 2000). Hill et al. (2009) compared the 1997/98 (Eastern) and 2002/03 (Dateline)
61 events searching for impacts over SA during the summer season. In their results the 1997/98 event
62 presented more intense precipitation in LPB, more intense subsidence over northern SA, a more
63 intense SALLJ, and a displaced Walker circulation over the ocean (Hill et al. 2011); these authors
64 further proposed the presence of a more intense Pacific South American (PSA) pattern. We focus
65 on the austral Spring because in this season the teleconnection between ENSO and LPB is best
66 established (Cazes-Boezio et al. 2003, Zamboni et al. 2011).

67 In developing the present analysis we found the need to develop an alternative criteria for iden-
68 tifying the different flavors of ENSO. This is described, along with our motivations, in Section 3.
69 In the following we outline as a background the methods employed in the literature.
70 Defining ENSO events is per se a challenge because every event presents somewhat different char-

71 acteristics regarding onset, duration, intensity. and evolution. Even the peak of the event, which
72 can largely be considered as locked to the seasonal cycle, has in the past occurred in seasons
73 other than the boreal winter (see e.g., Neelin et al. 2000, Xiao and Mechoso 2009). Indeed no
74 accepted definition of El Niño exists (Hanley et al. 2003), but noneless, different authors agree
75 on identifying a set of years as ENSO events (see Fu et al. 1986 and Larkin and Harrison 2005a
76 for comparisons among studies). Among these, Wang (1995) noticed that, contrary to what pre-
77 viously reported (Rasmusson and Carpenter 1982), SSTa of a group of El Niño first developed
78 in the central Pacific and appeared over the eastern Pacific only afterward (see Fig.3 in Wang
79 1995). Larkin and Harrison (2005a) compared 11 "conventionally identified" events occurred
80 since 1950 with a number of "additional" events ("Dateline" El Niño), resulting from the offi-
81 cial definition adopted by the USA National Oceanic and Atmospheric Administration (NOAA)
82 in 2003 (http://www.cpc.ncep.noaa.gov/products/analysis_monitoring/ensostuff/ensoyears.shtml).
83 Ashok et al. (2007) named the second Emipirical Orthogonal Function (EOF) analysis of Pacific
84 SSTs obtained from 1979-2004 "Modoki El Niño". Unlike other studies, these authors included an
85 area over the far western Pacific (125-145 E;10S-20N) to define an index for the Modoki events,
86 although the anomalies in this area are not pronounced (see their Fig. 2b). A similar but more
87 extended analysis by Kao and Yu (2009), who also identified an "Eastern" and "Central" El Niño,
88 shows minor anomalies over the same area, which we conclude do not reflect a significant fea-
89 ture of the new flavor. Further, the index Ashok et al. (2007) introduced cannot be employed to
90 cathegorize all ENSO events; for example, it would miss the El Niño event of 1997 (the El Niño
91 Modoki index was -0.53 during the austral Spring of that year). Other recent definitions are based
92 on large anomalies in the Nino4 region from September through February ("Warm Pool" El Niño
93 of Kug et al. 2009), the onset of the events ("Spring" and "Summer" types of Xu and Chan 2001),
94 EOF and cluster analysis of Pacific SSTs ("Eastern" and "Central" SSTa of Kao and Yu 2009). Fu
95 et al. (1986) emphasized the importance of the zonal SSTa gradient in determining atmospheric
96 circulation changes.

97 One relevant aspect in the context of the ENSO flavors is their association with the decadal
98 variability. A simple examination of the events we considered do indeed suggest a higher (lower)
99 occurrence of Dateline (Eastern) events since the 1970s (see Table 2). Changes in the interannual
100 variability (Trenberth and Stepaniak 2001), duration, onset, intensity (Kao and Yu 2009), and per-
101 sistence (Yu and Kao 2007) of SSTa in different areas of the tropical Pacific have been reported, as
102 well as associations with interdecadal changes in the northern tropical Pacific (Zhang et al. 1997),
103 the Pacific Decadal Oscillation (Hanley et al. 2003), and its relationship with precipitation in SA

104 (Kayano and Andreoli 2007). While research continues to add to our understanding of this aspect,
105 we seek to elucidate the possible different impacts of ENSO flavors over LPB so as to anticipate
106 considerations regarding decadal variation over the region and predictability.

107 In sorting past events, we noticed the existence of a pattern that, to the best of our knowledge, has
108 not previously reported. This consists of approximately uniform SSTa from the South American
109 coast to the central Pacific, and to which unexpected precipitation anomalies in SA correspond
110 (see Fig. 3).

111 We start by discussing our method for sorting the different flavors, whose corresponding pre-
112 cipitation and circulation characteristics are contrasted. Next, we discuss the dynamics of the
113 different flavors using idealized and AMIP-type of experiments with the International Centre for
114 Theoretical Physics Atmospheric General Circulation Model (ICTP AGCM) (previously named
115 SPEEDY) (Molteni 2003) and ECHAM4 (Roeckner et al. 1996). The paper is organized as fol-
116 lows. Section 2 describes the datasets we use. In Section 3 we discuss our definition of the flavors.
117 Section 4 compares observations and reanalysis data. Section 5 describes the models' response to
118 idealized experiment in which sintetic SSTa mimic the flavors. These results are then compared
119 in Section 6 with those obtained with AMIP types of experiments. We present observational evi-
120 dences of a tropical influence (Gill type of response) on precipitation in LPB in Section 7, and we
121 conclude in Section 8 with a summary of our findings.

122 **2 Datasets, numerical models, and experiments**

123 In the present study we focus on the austral Spring, chosen as the average of October and Novem-
124 ber to represent the coherent signal throughout the season (Montecinos et al. 2000). The period
125 of interest is 1948-2002. Our analysis compares modeling results with available reanalysis and
126 observational datasets.

127 The Atmospheric General Circulation Models (AGCMs) we employed are ECHAM4 (Roeck-
128 ner et al., 1996) and the International Centre for Theoretical Physics (ICTP) AGCM (Molteni
129 , 2003). The ICTP AGCM is an intermediate-complexity model and includes physically based
130 parameterizations of large-scale condensation, shallow and deep convection, short-wave and long-
131 wave radiation, surface fluxes of momentum, heat and moisture, and vertical diffusion (see also
132 Kucharski et al, 2006). The ICTP AGCM has been employed in research on the South American
133 Monsoon (Barreiro and Tippmann 2008) and investigations on the link between the circulation in
134 the Southern Hemisphere and in SA (Zamboni et al. 2011). The configurations we used have a

135 spectral truncation at total wavenumber T106 and 19 sigma vertical levels for ECHAM4, while 8
136 vertical sigma levels and a horizontal resolution of T30 characterize the ICTP AGCM. We mainly
137 discuss results obtained with ECHAM4 since they better compare with observations, although the
138 ICTP AGCM provides similar dynamics (see Section 6).

139 The first set of experiments we present is intended to restrict the models' response to anomalies
140 in the tropical Pacific. These anomalies, both positive and negative, are imposed on the October-
141 November SST climatology and have a Gaussian shape with a maximum of 2°C (Fig. 2) centered
142 in three locations so as to mimic the ENSO flavors. The experiments, consisting of 30 year long
143 runs for ECHAM4 and 50 year runs for the ICTP AGCM, are then subtracted from a control
144 run performed with climatological SSTs to obtain anomalies. We refer to these experiments as
145 "idealized experiments". The second set consists of an Amip type ensemble, in which observed
146 interannually varying SSTs have been used as boundary conditions. The results we present are
147 obtained by averaging over a 9-member ensemble for ECHAM4 and a 35-member ensemble for
148 the ICTP AGCM; these members differ by the atmospheric initial conditions.

149 The global monthly sea surface temperature is taken from the HadISST dataset (Rayner et al.,
150 2003), which is available from 1871 to the present at a resolution of 1°.

151 The precipitation dataset we use was compiled by the Climate Research Unit (CRU), University
152 of East Anglia
153 (<http://www.cru.uea.ac.uk/cru/data/hrg.htm>), reconstructing monthly precipitation from gauge mea-
154 surements. Data are available at 0.5° x 0.5° horizontal resolution over land for the period 1901-
155 2002 (Mitchell and Jones, 2005). We additionally employ the Climate Prediction Center Merged
156 Analysis of Precipitation (CMAP) dataset (Xie and Arkin 1997) for guidance on precipitation pat-
157 terns over the oceans. The data are available for the period 1979-2009, which presents a limitation
158 since it covers our period of analysis only partially. This aspect is particularly severe for Eastern
159 La Niña and the flavor we named "Spread" (see Section 3), in fact all the events occurred before
160 1979 for the former and only 1 out of a total of 4 dates after 1979 for the latter.

161 The atmospheric fields correspond to the global National Centers for Environmental Prediction-
162 National Center for Atmospheric Research (NCEP-NCAR) reanalysis; these are available at 2.5°
163 x 2.5° horizontal resolution (Kalnay et al. 1996) from 1948 to the present.

164

165 **3 Definition of the events**

166 Our intention is to base the definition of Eastern and Dateline types of SSTa onto indices having
167 equal areal extension and together covering the entire eastern Pacific, from the South American
168 coast to the dateline. This is not possible, however, with the standard ENSO indices. Hence, we
169 introduce two new indices, Nino East (nE) and Nino West (nW), which consist of the average
170 standardized SSTa over 5S-5N; 170W-130W, 5S-5N; 120W-80W, respectively¹. These indices
171 measure the local *intensity* of SSTa, which must be a minimum of ± 0.5 in either nE or nW to
172 identify an ENSO event (Table 1). For comparison, anomalies are computed with respect to the
173 1971-2000 climatology and have the same persistence criteria as in the definition by NOAA. The
174 value of the indices in Spring is used to discriminate among the flavors. In fact, at the seasonal
175 scale the quick response of the atmosphere makes the simultaneous relationship between SSTa
176 and precipitation in LPB the strongest (Montecinos et al. 2000). The definitions of ENSO flavors
177 currently proposed in the literature are based on the onset of the events, EOF analysis, or indices
178 averaged over a season; none takes the view we propose.

179 The "Eastern El Niño" pattern is characterized by *larger* SSTa over the Eastern Pacific and
180 smaller or no anomalies over the Central Pacific; it represents the canonical ENSO. The location
181 of larger and smaller anomalies is reversed during "Dateline El Niño" events. To describe the
182 zonal gradient of SSTa we use a modified trans-Nino index (Trenberth and Stepaniak 2001) that
183 consists of the standardized difference between nE and nW, which we name Trans-Nino East-West
184 (TNIEW). We found a TNIEW equal to ± 0.3 suitable to discriminate among the flavors, while nE
185 or nW equal to 0.5 sets the threshold for the intensity (Table 1). Similar considerations hold for
186 La Niña but with the sign of anomalies reversed.

187 In analyzing the historical record of SSTs we noticed the existence of cases in which anoma-
188 lies were of approximately equal intensity from the eastern to the central tropical Pacific. Further
189 inspired by corresponding unexpected precipitation anomalies over SA (see Fig. 3), we decided
190 to conduct a separate analysis for this new flavor, which we named "Spread". To the best of our
191 knowledge, no similar patterns have been considered in the literature before.

192 We list in table 2 the events we consider, along with the composite of SSTa for each flavor in
193 Fig. 1.

194 One novel aspect of the present study is the investigation of La Niña events in the context of

¹The band 120W-130W is not represented by either nE or nW; this is chosen with the aim of reducing the sensitivity of the stratification arising from more westward extended Eastern ENSOs and more eastward extended Dateline ENSOs.

195 ENSO flavors, which previously were studied only for the austral summer (Cazes-Boezio, per-
196 sonal communication). A relevant consequence of our definition is the presence of "Eastern" La
197 Niña in our categories, which may be surprising since negative SSTa usually first develop over the
198 central Pacific. We point out that our method disregards the evolution of SSTa and is thus not nec-
199 essarily suitable to describe the ENSO phenomenon itself; rather, it is designed to explore impacts
200 simultaneous to the occurrence of ENSO. On the other hand, we believe that nE, nW, and TNIEW
201 may prove effective in explorations of the flavors regardless of the emphasis on the simultaneous
202 responses.

203

204 **4 Observations**

205 We begin our discussion by examining the effect on precipitation associated with the three fla-
206 vors (Fig. 3). This is substantially linear in both the sign and the intensity of SSTa for Eastern
207 and Dateline, in agreement with previous analyses (e.g., Grimm et al. 2000). In the remainder
208 of the paper we show composites of El Niño minus La Niña for these flavors, unless otherwise
209 stated. Substantially different features *locally* over SA distinguish the positive and negative phase
210 of Spread; we thus show them separately.

211 Eastern and Dateline feature increased loads over LPB and negative anomalies to the northeast,
212 forming the see-saw pattern known as the canonical response to ENSO over SA. The largest pre-
213 cipitation anomalies are found for Eastern, which may be the result of the outstanding intensity of
214 SSTa during 1982 and 1997.

215 Remarkably distinct patterns appear during Spread events (Fig. 3c): in both phases a wide
216 region of increased precipitation is located in place of the dry conditions observed for the other
217 flavors (50W-20S). These anomalies are statistically significant at the 95% level, as obtained by a
218 non-parametric test, based on a bootstrap procedure using a resampling technique (Wilks 1995).
219 Normal precipitation is found in LPB during Spread El Niño, while an east-west dipole character-
220 izes Spread La Niña.

221 Examination of reanalysis data for Eastern reveals the signature of a substantial Tropical heat-
222 ing over the central Pacific and the existence of a clear wavelike pattern in the South Hemisphere
223 arching from the Indian Ocean to eastern SA (Fig. 4a), which is recognized as the leading PSA
224 mode (Kidson 1988). This and in particular its eastern extension, the vortex centered at 20S-50W
225 has been linked to an increased and southeastward oriented SALLJ (Zamboni et al. 2010, Diaz

226 and Aceituno 2003), which in turn leads to increased precipitation over the subtropical regions and
227 opposite anomalies over the SACZ (Diaz and Aceituno 2003, Mo and Paegle 2001, Paegle and
228 Mo 2002). The chain of elements we have just sketched represents the mechanism for the impact
229 of ENSO when all past events are considered together (Zamboni et al. 2011).

230 Upper level circulation anomalies for Dateline are similar to those of Eastern but less intense
231 (Fig. 4b). In the Southern Hemisphere a wave train is evident, but anomalies between 120E and
232 180E are much less pronounced compared with those to the east. These appear the result of an ad-
233 ditional wave that propagates meridionally from the central Pacific (Vera et al. 2004) and merges
234 with the PSA at 120W-70S. A clear vortex is also evident over subtropical SA.

235 A circulation of smaller intensity is found for Spread, particularly over the central Pacific in the
236 Northern Hemisphere (Figs. 4c,d). In the Southern Hemisphere, anomalies recall the PSA pattern,
237 but opposite anomalies occur at very high latitudes and possibly interfere with the former. Of
238 interest to our goals, the anticyclonic circulation over eastern SA is displaced over the Atlantic it
239 influences SA only marginally during La Niña (Fig. 4d), while it is flanked by a large-scale cy-
240 clone during El Niño (Fig. 4c). At low levels an intense cyclone is found inland over northern SA
241 during El Niño, while an opposite westerly flow at 20S characterizes La Niña, consistently with
242 respectively enhanced and reduced SALLJ toward the region of intense precipitation anomalies
243 along the coast.

244 Observed SSTa of the three flavors differ in relevant aspects beyond their location and hence
245 limit the extent to which a direct comparison can be carried out. For example SSTa over the trop-
246 ical Pacific during Eastern are 30% larger than those of the other flavors. As mentioned earlier,
247 only three events represent the positive phase of this flavor, and thus results might depend on the
248 specific features of these. Additionally, the belt of opposite anomalies in the subtropical Pacific,
249 which is part of the ENSO dynamics, has been suggested as a key factor for the propagation of
250 the PSA (Vera et al. 2004) and are for Spread barely noticeable. SSTa in other basins introduce
251 further dissimilarities among the flavors; examples are found in the Indian and southern Atlantic
252 Oceans for Eastern and in the tropical Atlantic for Spread (see Fig. 1).

253 To conduct a systematic investigation and focus on the response from the Pacific Ocean we per-
254 formed a number of idealized experiments in which SSTa mimicing the three flavors (Fig. 1) have
255 been superimposed onto the ON climatology in two AGCMs. We analyze these in the following
256 section. The results are then compared with those obtained with AMIP types of simulations in
257 section 6 to investigate the response of the models to realistic SSTs, as well as the role of SSTa in
258 other oceans.

259 **5 Idealized experiments**

260 The response of Echam to Eastern types of idealized SSTa consists of several of the features we
261 have described in section 4, namely, the PSA, and anomalous SALLJ and precipitation anomalies
262 in LPB. Clearly, the tropical Pacific accounts for much of the response we see in the observations.
263 Of further interest is the presence of an intense Gill quadrupole (Gill 1980), whose anomalous
264 vortices are located above the SSTa (Fig. 5) and over the tropical Atlantic Ocean, the latter be-
265 ing of smaller intensity. The circulation associated with positive SSTa is indicative of low level
266 anomalous westerlies over the tropical Pacific and easterlies over the Atlantic, which thus appear
267 to contribute in increasing precipitation over LPB via enhancement of the SALLJ (Fig.5c). Over
268 the eastern Pacific Ocean around 30S, the baroclinic response over the tropics is accompanied by
269 a barotropic wave propagating meridionally (Fig.5a,b). This is possibly generated by the vortic-
270 ity source corresponding to the heating induced by tropical SSTa and intense precipitation there
271 (Sardeshmukh and Hoskins 1985) and resembles the secondary wave discussed in section 4. To
272 the east the interference of such a wave with the PSA is also evident.

273 The higher sensitivity of the atmosphere to SSTa located over the central Pacific determines
274 a stronger atmospheric response² for Dateline, resulting in more intense Gill's quadrupole and
275 wave trains. Precipitation anomalies in SA are reproduced by the AGCM only for positive SSTa
276 and over LPB. The difficulty in reproducing precipitation anomalies with a climate model is well
277 known, and we thus continue our analysis on the more reliable dynamical fields. The dynamics
278 of the response over SA consists of a pure PSA³ south of 45S, while to the north at low levels a
279 broad anticyclonic circulation results from the combination of the vortex (Fig. 5e) and of a baro-
280 clinic circulation over the tropical Atlantic (Figs. 5d,e). This joint effect leads to an intense SALLJ
281 and positive precipitation over LPB (Fig. 5f). The mechanism linking the canonical ENSO to
282 precipitation anomalies in LPB is thus found even when positive SSTa are located over the central
283 Pacific. For negative SSTa the expected cyclone over SA is lacking, as are precipitation anomalies
284 over subtropical SA (Fig. 6, upper panels), while a wave train propagating from the tropics is
285 present. The nonlinearity of the formation of the vortex over SA to the sign of SSTa appears to be
286 an artifact of this idealized experiment, as it is not present in either the observations or the Amip
287 experiments (see Section 6). The presence of a Gill response is also found for Dateline.

²In fact, the actual temperature is higher.

³The wave train on the middle left panel of Fig. 5 could also be interpreted as the wave propagating directly from the location of SSTa. However, the arching pattern and the location of anomalies remarkably correspond to those of the PSA and PNA. The same consideration holds for Spread.

288 For Spread the Gill’s quadrupole is zonally elongated (as SSTa are) and spans the entire tropical
289 Pacific (Figs. 5g,h); this appears to interfere with the intensity of the PSA, whose anomalies result
290 dumped. Nevertheless, anomalies associated with the PSA and Pacific North American patterns are
291 approximately on the same locations as those of Dateline (Fig. 5d,g), supporting the interpretation
292 that these patterns are resonant modes of the system (Robertson and Mechoso 2003) rather than
293 propagating waves dependent on the precise location of their source. Corresponding to positive
294 SSTa, precipitation anomalies in the model are the result of the Gill response alone, with the PSA
295 pattern being confined at high latitudes, since its eastern end is lacking. Indeed, such a vortex may
296 be independent of the PSA (Zamboni et al. 2011). Although at high latitudes Spread does not
297 present the PSA for negative SSTa, but a zonal belt of alternate anomalies, it features a cyclonic
298 circulation at 30S that, together with the circulation associated with the Gill response to the north,
299 creates a precipitation dipole with centers over LPB and SACZ (Fig. 6, bottom panels). The ideal-
300 ized experiment clearly misses the precipitation patterns characterizing Spread in the observations
301 and produces a similar mechanism found for the other flavors.

302 Summarizing, in the idealized experiments, a combination of the canonical mechanism (PSA
303 and the presence of a vortex over subtropical SA) and the Gill response we have documented
304 determine the impact on precipitation over LPB for Eastern and the positive phase of Dateline.
305 We highlighted the leading role of the tropical Pacific in shaping the atmospheric response and the
306 capability of the model in reproducing a number of dynamical features, as well as anomalies of
307 smaller intensity during La Niña for all flavors. On the other hand, we cannot draw firm conclu-
308 sions on what determines the patterns of precipitation in LPB for Spread and Dateline La Niña,
309 the origin of the PSA pattern, and the occurrence of the vortex over SA. Clearly, further elements,
310 not reproduced by the idealized experiments, determine these features. We address these aspects
311 in the next section, discussing in particular the sources of the PSA and their reproducibility with
312 an AGCM.

313 The Gill response we documented motivated us to explore whether it is a real feature of the
314 circulation (instead of a model’s artifact) and the extent to which it influences circulation and
315 precipitation over subtropical SA. We discuss this aspect in Section 6 using Amip types of exper-
316 iments; while in Section 7 we show its existence in the observations.

317 6 Amip experiments and discussion

318 In this section we explore the role of SSTa other than those in the tropical Pacific and draw con-
319 siderations about the capability and limitations of an AGCM in reproducing the dynamics of the
320 flavors, as well as their impact on precipitation in LPB. To this end, we compare results obtained
321 with the idealized and Amip experimentsa and support the novel results we document with both
322 ECHAM4 and the ICTP AGCM. In this regard results from the two AGCMs present only minor
323 differences; and although we considered them both to corroborate our conclusions, it would be
324 redundant to show the results for the ICTP AGCM with additional detail.

325 The dynamics and response for Eastern El Niño are similar between the idealized and Amip
326 experiments (Figs. 7a,b), confirming that the model's response is largely driven by the tropical
327 Pacific. The Gill response is less intense and more extended into the central Pacific during El Niño
328 in the Amip experiment (Figs. 7a,b); a more marked PSA pattern is also present and compares
329 remarkably well with the observations (Fig. 4a). Similar to the observations, but not the idealized
330 experiments, opposite precipitation anomalies accompanied by upper-level divergence (conver-
331 gence) are found over the eastern and central (western) Pacific (Fig.7c). This difference between
332 the Amip and idealized experiments suggests that even though the largest SSTa are located over
333 the east during Eastern, the more extended pattern into the central Pacific, featured in the obser-
334 vations but not in the idealized experiments, plays a key role in shaping the Walker circulation.
335 We posit that the upper-level divergence over the central Pacific induces dry conditions and upper-
336 level convergence at 120E, which in turn establishes the PSA, in agreement with the Rossby waves
337 sources (RWS) we explored⁴. For example, during Eastern La Niña the Amip experiment does not
338 present either the PSA or the upper level divergence at 120E (Fig. 7d). As in the observations, the
339 AGCMs we employed do reproduce a smaller response during La Niña, but they require stronger
340 SSTa to trigger the PSA, while a clear wave emanated from the central Pacific is evident in the
341 Amip experiment. The asymmetry in the response for the two phases of Eastern may originate
342 over the western Pacific between 150W and 180W, a region in which SSTa of Eastern La Niña
343 are substantially less intense than those of El Niño. The lack of a corresponding well-reproduced
344 precipitation pattern over the western Pacific and Indian Ocean is a general drawback of current
345 AGCMs, and it is due to the lack of atmosphere-ocean feedbacks over the region in this type of
346 experiments. The lack of positive SSTa over the subtropics in the southern Pacific during La Niña
347 can also play a role (Vera et al. 2004).

⁴In the following we show precipitation patterns since the patterns of RWS are noisy.

348 For Dateline the upper-level divergence is less intense in the Amip experiments (Fig. 8), con-
349 verge to the west is minor, and the PSA is absent, different from the marked extratropical tele-
350 connection seen in the idealized experiments (Fig. 5d). The precipitation pattern over the central
351 and western Pacific is similar for Eastern and Dateline in both the Amip experiment (Fig. 7c and
352 Fig. 8c) and the observations (Fig. 9), but the intensity of both SSTa and precipitation anomalies
353 is double for Eastern. Comparing the SST patterns, one can see that anomalies for Eastern and
354 Dateline are similar over the central Pacific, while larger anomalies exist to the east for Eastern.
355 We conclude that the largest response during Eastern is determined by the outstanding intensity of
356 a wide, zonally extended pattern of SSTa. In the subtropics over the Pacific, SSTa are substantial
357 during Dateline, and we thus deduce that their role in determining the PSA is significantly minor
358 compared with that of the *intensity* of SSTa over the tropics.

359 Dateline also features a wave extending meridionally from the tropics for both El Niño (Fig. 8)
360 and La Niña (not shown); a result that is also obtained with the ICTP AGCM (Fig. 10a).

361 We anticipated in Section 5 the presence of the vortex over SA only in the Amip experiment for
362 Dateline La Niña. As discussed, we found that the Gill response tends to be too strong and merid-
363 ionally extended in the idealized experiments, while it is significantly less intense in the Amip
364 experiments, especially to the east for both ECHAM (Fig. 8) and the ICTP AGCM (Fig. 10).
365 Nevertheless, its influence on the SALLJ (Fig. 8c) and thus precipitation in LPB are recognized.

366 The dynamics for Spread El Niño is the same for the two experiments, but anomalies are smaller
367 in the Amip, in particular, no precipitation anomalies appear over SA (not shown). The AGCMs
368 produce no significant anomalies in the extratropics, a feature possibly indicative of an excessively
369 strong atmospheric response to zonally extended SSTa. As already noticed, the models' response
370 to La Niña is smaller over the tropics, and the Amip experiment produces circulation anomalies in
371 the extratropics and the secondary wave (Fig. 8). However, the model proposes the same dynamics
372 as for the other flavors and anomalies substantially different from those seen in the observations.

373 **7 Role of the Gill response in precipitation in LPB**

374 In the previous sections we discussed the influence of a Gill type of response on precipitation over
375 LPB we saw in the modeling experiments we conducted. The latter accompanies the more docu-
376 mented Gill response found to the west of SSTa and consists of upper level cyclonic (anticyclonic)
377 vortices to the *east* of positive (negative) SSTa. At low levels it strenghtens (reduces) the trade
378 winds over the Atlantic and consequently the intensity of the SALLJ toward LPB. In this section

379 we show evidence of this circulation in the observations.

380 Examination of the eddy streamfunction at different vertical levels shows for Eastern the two
381 anticyclonic vortices straddling the equator over the eastern Pacific, typical of the Gill response,
382 from 400 mb (Fig. 11a) and above. Over the same range of altitudes two less intense cyclonic vor-
383 tices are present at 80W-5S and 15N, which may indeed represent the circulation we are seeking.
384 Above 400 mb, the signal strengthens (not shown). At lower levels the circulation is opposite; and
385 although patterns are less neat, two anticyclonic circulations are present at 60W-10S and 10N. The
386 eastern component of the Gill response is found to have smaller intensity in both the numerical
387 experiments and in the observations, which is expected because of the competing signal sourced in
388 the Atlantic Warm Pool. The Amazon also represents an important source of heating; and since its
389 role cannot be represented in an Amip experiment, a model including dynamic vegetation would
390 elucidate this aspect. A dumping of the southeastern vortex of the Gill response by the barotropic
391 vortex over subtropical SA is also plausible for Eastern since the latter extends into tropical lati-
392 tudes.

393 For Dateline two zonally extended cyclones are present at 400 mb at tropical latitudes on either
394 side of the equator between 80W-40W (Fig. 11c), while at low levels a vortex is present at 10N-
395 80W but not to the south. Hence, for this flavor, the impact of the Gill response on circulation over
396 tropical SA is minor (Figs. 11c,d).

397 During Spread El Niño an intense low-level anticyclone at 15S-50W diverts the SALLJ toward
398 northeastern Brazil, where a region of convergence is found (Fig. 12a). The same rotation is
399 visible up to 500 mb (not shown). We interpret the remarkable intensity and extension of this
400 vortex as the result of the Gill response and local forcings. In exploring this aspect we suggest
401 investigating the role of local effects, for example, vegetation and soil moisture, which have been
402 shown to impact the local circulation during ENSO (Grimm et al. 2007). At upper levels a cy-
403 clone is present at 60W-10N, consistently with a Gill response, but to the south the other pole is
404 destroyed (Fig. 12c). The latter is possibly overcome by the cyclonic circulation associated with
405 the secondary wave at 30-40S; 60W (Figs. 12b,c). The reasons behind the presence of such a
406 strong signal remain unclear at present.

407 A small vortex at 10-20N; 60W during Spread La Niña is seen throughout the atmospheric col-
408 umn (Fig. 12). An opposite circulation is detected at 400 mb across SA over 10S, but at upper
409 levels the latter circulation is then overcome by the increased effect of the cyclone over subtropical
410 SA (Figs. 12e,f).

411 A number of features differentiates Spread from Eastern and Dateline and its lack of linearity

412 between the positive and negative phases. Local effects appear to have played a relevant role in
413 shaping precipitation and circulation anomalies during these past events. Land processes, which
414 could not be exploited by the experiments we conducted but likely are important at the beginning
415 of the rainy season in northern SA, deserve more attention in future studies. On the other hand,
416 anomalies associated with the secondary wave are remarkably zonally extended over the subtrop-
417 ics at upper levels during Spread. These appear to influence the circulation over SA directly rather
418 than via an extratropical connection as it is for Dateline.

419 **8 Summary**

420 In this paper we have explored to what extent precipitation anomalies in La Plata Basin (LPB)
421 during the Spring season are sensitive to SSTa located in different areas of the tropical Pacific.
422 In these patterns of SST, referred to in the literature as ENSO flavors, the largest anomalies are
423 located over the east or around the dateline during Eastern and Dateline events, respectively.

424 We introduced three indices representing the areal average of SSTa over the eastern (nE), the
425 central Pacific (nW) and their difference (TNIEW) to quantify the intensity and zonal gradient
426 of SSTa, respectively. These indices are more suitable for investigations of ENSO flavors since
427 they cover areas of equal extension in the region where larger SSTa occur, a goal that cannot be
428 achieved with the standard El Niño indices (see Section 3).

429 In investigating the events occurred during 1948-2002, we noticed the existence of SST patterns
430 in which anomalies have a uniform intensity from the eastern to the central Pacific; we named this
431 new flavor Spread (Fig. 1). An additional novel aspect of the present study is the analysis of La
432 Niña, since investigations in the context of the flavors have so far focused on El Niño only.

433 To conduct this research, we employed observational and reanalysis data as well as numerical
434 experiments performed with two AGCMs. We realized a set of idealized experiments in which
435 SSTa mimicing of the flavors have been superimposed to the climatology for ON first; then we
436 performed a set of Amip type of experiments aimed to determine the relative role of SSTa over the
437 Pacific and other basins.

438 Contrary to our expectations, we found a similar precipitation pattern for the Eastern and Date-
439 line flavors. This consists of increased precipitation over LPB and decreased precipitation to the
440 north over the SACZ; the pattern reverses during La Niña. These results are comparable to those
441 obtained by Hill et al. (2011) for the summer season. Particularly relevant precipitation anomalies
442 during Spread consist of positive loads in place of dry conditions occurring for the other flavors at

443 20S along the Atlantic coast of SA (Fig. 3).

444 Precipitation anomalies in LPB are linked to the circulation upstream, namely, the Pacific-South
445 American Mode (PSA; Mo and Paegle 2001, Casez-Boezio et al. 2003, Paegle and Mo 2002),
446 whose establishment occurs via reduced precipitation and upper-level convergence over the west-
447 ern Pacific, which is in turn driven by convection over the central Pacific. Keys in driving the
448 anomalous Walker circulation are SSTa between 150W and 180W but also intense anomalies over
449 the eastern Pacific when anomalies are present over the central Pacific. Further, the intensity of
450 SSTa, rather than their location or the presence of opposite anomalies in the subtropics (Vera et al.
451 2004) is the leading factor in determining the response.

452 Corresponding to intense SSTa extended into the central Pacific, as for example during the event
453 of 1982 and 1997, we found the AGCMs we employed were able to reproduce the PSA and the
454 pattern of precipitation over the ocean partially. However, this is not the case when smaller SSTa
455 occur and reveal the importance of the atmosphere-ocean interaction occurring there.

456 We documented the existence of an additional wave train emanated from the region of the main
457 heating. This is noticed in the observed past events and is reproduced in the modelling experiments
458 we performed. Such a wave train, first documented by Vera et al.(2004), has a strong meridional
459 propagation, is present during Dateline, and is prominent during Spread. During Spread, it ap-
460 pears so intense that it modifies the extratropical connection by shifting it to the north at 120W,
461 while during Dateline a clear interference with the PSA occurs east of 120W (Fig. 4). Further
462 explorations would benefit our understanding of its interaction with the PSA, the formation of the
463 vortex over subtropical SA, and thus precipitation anomalies over LPB.

464 Locally over SA circulation anomalies are driven by the presence of a continental-scale vortex,
465 which is often, but not always, the eastern end of the PSA (Zamboni et al. 2011). This vortex is
466 present for all flavors, but relevant variations in its position are not accounted for by SSTa. Rather,
467 local effects may play an important role and deserve more investigation, for example by using of
468 a model with dynamic vegetation. Further, the vortex over SA and an intense SALLJ are found
469 even when the PSA is not, for example during Dateline events (see Fig. 4), suggesting that the
470 secondary wave can also trigger their occurrence.

471 The idealized experiments suggest the existence of a Gill type of response to the east of the heat-
472 ing region, with effects impacting the circulation locally over SA and thus precipitation over LPB.
473 To our knowledge, this mechanism has never been reported in the literature. We thus searched for
474 this signal in the observed past events and indeed found proof of its existence (see Section 7). The
475 intensity of the vortices to the east of the heating region is significantly smaller in the observations

476 than in the model, especially at low levels, but it still appears to influence precipitation via modu-
477 lation of the intensity of the SALLJ for Eastern. No significant anomalies are found at low levels
478 for Dateline, whereas the circulation for Spread is particularly strong and thus possibly amplified
479 by local effects. Indeed, our modeling experiments provide an overly strong response to El Niño,
480 while the same response seen for the other flavors corresponds to that of Spread La Niña. We
481 emphasize the need for exploring these local impacts to fully identify the intensity of these versus
482 remote forcing; investigations with a model with dynamic vegetation would be beneficial.

483 *Acknowledgements.* The research leading to these results has received funding from the European Com-
484 munity's Seventh Framework Programme (FP7/2007-2013) under Grant Agreement N° 212492 (CLARIS
485 LPB. A Europe-South America Network for Climate Change Assessment and Impact Studies in La Plata
486 Basin). The authors are grateful to the colleagues of the WP4 "Hydroclimate past and future low-frequency
487 variability, trends and shifts" for useful discussions during the project's first Annual Meeting, February
488 2010, in Rome, Italy, and at The Meeting of the Americas, August 2010, in Foz do Iguaçu, Brazil.
489 This work was partially supported by American Recovery and Reinvestment Act (ARRA) funding through
490 the Office of Advanced Scientific Computing Research, Office of Science, U.S. Dept. of Energy, under
491 Contract DE-AC02-06CH11357 and by the U.S. Department of Energy, Basic Energy Sciences, Office of
492 Science, under contract # DE-AC02-06CH11357.

493 **References**

- 494 Aceituno, P. (1988) On the Functioning of the Southern Oscillation in the South American Sector. Part I:
495 Surface Climate. *Mon. Wea. Rev.*, 116: 505-524.
- 496 Ashok, K., Behera, S. K., Rao, S. A., Weng, H. Y. and Yamagata, T. (2007) El Niño Modoki and its possible
497 teleconnection. *Journal of Geophysical Research-oceans*, 112
- 498 Barreiro, M. and A. Tippmann (2008) Atlantic Modulation of El Niño Influence on Summertime Rainfall
499 over Southeastern South America. *Geophys. Res. Lett.*, 35, L16704, doi:10.1029/2008GL035019.
- 500 Cazes-Boezio, G., A.W. Robertson, and C.R. Mechoso (2003) Seasonal Dependence of ENSO Teleconnec-
501 tions over South America and Relationships with Precipitation over Uruguay. *J. Climate*, 16: 1159-1176.
- 502 Diaz, A., and P. Aceituno (2003) Atmospheric Circulation Anomalies during Episodes of Enhanced and
503 Reduced Convective Cloudiness over Uruguay. *J. Climate*, 16, 3171-3185.
- 504 Feng, J., and J. Li (2011) Influence of El Niño Modoki on Spring Rainfall over South China. *J. Geophys.*
505 *Res.*, 116, D13102, doi:10.1029/2010JD015160.
- 506 Ferreira, R.N., T.M. Rickenbach, D.L. Herdies, and L.M.V. Carvalho (2003) Variability of South American
507 Convective Cloud Systems and Tropospheric Circulation during January - March 1998 and 1999. *Mon.*
508 *Wea. Rev.*, 131, 961- 973.
- 509 Fu, Congbin, H. F. Diaz, J. O. Fletcher, (1986) Characteristics of the Response of Sea Surface Temperature
510 in the Central Pacific Associated with Warm Episodes of the Southern Oscillation. *Mon. Wea. Rev.*, 114,
511 1716 -1739.
- 512 Gill, A. E. (1980) Some Simple Solutions for Heat-Induced Tropical Circulation. *Quarterly Journal of the*
513 *Royal Meteorological Society*, 106: 447-462. doi: 10.1002/qj.49710644905
- 514 Grimm, A.M., V.R. Barros, and M.E. Doyle (2000) Climate Variability in Southern South America Associ-
515 ated with El Niño and La Niña Events. *J. Climate*, 13: 35-58.
- 516 Grimm, A.M., S.E.T. Ferraz, and J. Gomes (1998) Precipitation Anomalies in Southern Brazil Associated
517 with El Niño and La Niña Events. *J. Climate*, 11: 2863-2880.
- 518 Hanley, D. E., M. A. Bourassa, J. J. O'Brien, S. R. Smith, E. R. Spade (2003) A Quantitative Evaluation of
519 ENSO Indices. *J. Climate*, 16, 1249-1258.
- 520 Hill, K. J., A. S. Taschetto, and M. H. England (2009) South American Rainfall Impacts associated with
521 Inter-El Niño Variations. *Geophys. Res. Lett.*, 36, L19702, doi:10.1029/2009GL040164.
- 522 Hill, K. J., A. S. Taschetto, and M. H. England (2011) Sensitivity of South American Summer Rainfall to
523 Tropical Pacific Ocean SST Anomalies. *Geophys. Res. Lett.*, 38, L01701, doi:10.1029/2010GL045571
- 524 Kalnay E., Kanamitsu M., Kistler R., and co-authors (1996) The NCEP/NCAR 40-Year Reanalysis Project.
525 *Bull. Am. Meteor. Soc.* 77 437-471.
- 526 Kao, H. and J. Yu, (2009) Contrasting Eastern-Pacific and Central-Pacific Types of ENSO. *J. Climate*, 22,
527 615632.
- 528 Kayano, M. T. and Andreoli, R. V. (2007) Relations of South American Summer Rainfall Interannual

529 Variations with the Pacific Decadal Oscillation. *International Journal of Climatology*, 27: 531-540. doi:
530 10.1002/joc.1417.

531 Kidson, J.W. (1988) Interannual Variations in the Southern Hemisphere Circulation. *J. Climate*, 1, 1177-
532 1198.

533 Kucharski F., Molteni F., and Yoo J.H. (2006) SST Forcing of Decadal Indian Monsoon Rainfall Variability.
534 *Geophys. Res. Lett.* 33: L03709 DOI: 10.10029/2005GL025371

535 Kug, J.-S., F.F. Jin, and S. An (2009) Two Types of El Niño Events: Cold Tongue El Nio and Warm Pool
536 El Niño. *J. Climate*, 22, 1499-1515.

537 Larkin, N. K. and Harrison, D. E. (2005a) Global Seasonal Temperature and Precipitation Anomalies during
538 El Niño Autumn and Winter. *Geophysical Research Letters*, 2005, 32, L16705

539 Larkin, N. K., and D. E. Harrison (2005b) On the Definition of El Niño and Associated Seasonal Average
540 U.S. Weather Anomalies, *Geophys. Res. Lett.*, 32, L13705, doi:10.1029/2005GL022738.

541 Liebmann B., Kiladis G.N., Vera C.S., Saulo A.C., and Carvalho L.M.V. (2004) Subseasonal Variations of
542 Rainfall in South America in the Vicinity of the Low-Level Jet East of the Andes and Comparison to
543 Those in the South Atlantic Convergence Zone. *J. Climate*, 17: 3829-3842.

544 Mitchell, T.D. and Jones P.D. (2005) An Improved Method of Constructing a Database of Monthly Climate
545 Observations and Associated High-Resolution Grids. *Int J. Climatol.*, 25, 693-712.

546 Mo, K. C. (2010) Interdecadal Modulation of the Impact of ENSO on Precipitation and Temperature over
547 the United States. *Journal of Climate*, 23, 3639-3656

548 Mo, K.C. and J.N. Paegle (2001) The Pacific-South American Modes and their Downstream Effects. *Int. J.*
549 *Climatol.*, 21, 1211-1229.

550 Molteni, F. (2003) Atmospheric Simulations Using a GCM with Simplified Physical Parametrizations, I:
551 Model Climatology and Variability in Multi-Decadal Experiments. *Clim. Dyn.* 20:175-191.

552 Montecinos, A., A. Diaz, and P. Aceituno (2002) Seasonal Diagnostic and Predictability of Rainfall in
553 Subtropical South America Based on tropical Pacific SST. *J. Climate*, 13: 746-758.

554 Neelin, J.D., F.-F. Jin, and H.-H. Syu (2000) Variations in ENSO Phase Locking. *J. Climate*, 13, 2570-2590.

555 Paegle, J.N. and K.C. Mo (2002) Linkages between Summer Rainfall Variability over South America and
556 Sea Surface Temperature Anomalies. *J. Climate*, 15,1389-1407.

557 Rao, V. B. and K. Hada (1990) Characteristics of Rainfall over Brazil: Annual Variations and Connections
558 with the Southern Oscillation, *Theor. Appl. Climatol.*, 42: 81-91.

559 Rasmusson, E. M., and T. H. Carpenter (1982) Variations in Tropical Sea Surface Temperature and Surface
560 Wind Fields Associated with the Southern Oscillation/El Niño. *Mon. Wea. Rev.*, 110, 354-384.

561 Rayner N.A., Parker D.E., Horton E.B., Folland C.K., Alexander L.V., Rowell D.P., Kent E.C., and Kaplan
562 A. (2003) Global Analysis of Sea Surface Temperature, Sea Ice and Night Marine Air Temperature since
563 the Late Nineteenth Century. *J. Geophys. Res.* 18(D14) 4407 DOI:10.1029/2002JD002670

564 Robertson, A.W., and C.R. Mechoso (2003) Circulation Regimes and Low-Frequency Oscillations in the
565 South Pacific Sector. *Mon. Wea. Rev.*, 131, 1566-1576.

566 Roeckner, E., K. Arpe, L. Bengtsson, M. Christoph, M. Claussen, L. Dümenil, M. Esch, M. Giorgetta, U.
567 Schlese, and U. Schulzweida (1996) The Atmospheric General Circulation Model ECHAM4: Model
568 Description and Simulation of Present-Day Climate: *Max-Planck Institut für Meteorologie*, Report no.
569 218, Hamburg, 86 pp.

570 Sardeshmukh, P. D. and Hoskins, B. J. (1985) Vorticity Balances in the tropics during the 1982-83 El Niño-
571 Southern Oscillation Event. *Quarterly Journal of the Royal Meteorological Society*, 111: 261-278. doi:
572 10.1002/qj.49711146802.

573 Silva, G. A. M., Ambrizzi, T., and Marengo, J. A. (2009) Observational Evidences on the Modulation of
574 the South American Low Level Jet East of the Andes According the ENSO Variability, *Ann. Geophys.*,
575 27, 645-657.

576 Trenberth, K. E. and D.P. Stepaniak (2001) Indices of El Niño Evolution. *J. Climate*, 14, 1697-1701.

577 Wang B., (1995) Interdecadal Changes in El Niño Onset in the Last Four Decades. *J. Climate*, 8, 267285.

578 Wang, G. and Hendon, H. H. (2007) Sensitivity of Australian Rainfall to inter-El Niño Variations. *Journal*
579 *of Climate*, 20, 4211-4226.

580 Weng, H., Ashok, K., Behera, S. K., Rao, S. A. and Yamagata, T. (2007) Impacts of Recent El Nino Modoki
581 on Dry/Wet Conditions in the Pacific Rim during Boreal Summer. *Climate Dynamics*, 29, 113-129.

582 Wilks, D.S., 1995: *Statistical Methods in the Atmospheric Sciences*. Academic Press, 467 pp.

583 Xiao, H. and C. R. Mechoso (2009) Seasonal Cycle-El Nino Relationship: Validation of Hypotheses. *J.*
584 *Atmos. Sci.*, 66(6), 1633-1653.

585 Xie, P., and P.A. Arkin (1997) Global Precipitation: A 17-Year Monthly Analysis based on Gauge Obser-
586 vations, Satellite estimates, and Numerical Model Outputs. *Bull. Amer. Meteor. Soc.*, 78, 2539-2558.

587 Xu, J., and J. C. L. Chan (2001) The Role of the Asian-Australian Monsoon System in the Onset Time of
588 El Niño Events. *J. Climate*, 14, 418433.

589 Yu, J.-Y. and H.-Y. Kao, (2007) Decadal Changes of ENSO Persistence Barrier in SST and Ocean Heat Con-
590 tent Indices: 1958-2001. *Journal of Geophysical Research*, 112, D13106, doi:10.1029/2006JD007654.

591 Vera, C., G. Silvestri, V. Barros, A. Carril (2004) Differences in El Nio Response over the Southern Hemi-
592 sphere. *J. Climate*, 17, 1741-1753.

593 Zamboni L., F. Kucharski, and C.R. Mechoso (2011) Seasonal Variations of the Links Between the Interan-
594 nual Variability of South America and the South Pacific. *Climate Dynamics*. DOI: 10.1007/s00382-011-
595 1116-z

596 **Tables**

	El Niño	La Niña
Eastern	$TNIEW > 0.3$ $nE > 0.5$	$TNIEW < -0.3$ $nE < -0.5$
Dateline	$TNIEW < -0.3$ $nW > 0.5$	$TNEW < 0.3$ $nW < -0.5$
Spread	$-0.3 < TNIEW < 0.3$ $nE > 0.5$ $nW > 0.5$	$-0.3 < TNIEW < 0.3$ $nE < -0.5$ $nW < -0.5$

Table 1. Definition of ENSO flavors.

	Eastern	Dateline	Spread
El Niño	1951, 1982, 1997	1963, 1965, 1968 1977, 1986, 1987, 1991, 1994, 2002	1957, 1969, 1972, 1976
La Niña	1949, 1950, 1954, 1955 1970, 1971	1964, 1973, 1975, 1988, 1995, 1998	1956, 1974, 1984, 1999, 2000

Table 2. ENSO flavors events for 1948-2002.

597 **Figure Captions**

Fig. 1. Composite of observed SSTa ($^{\circ}\text{C}$) for Eastern (upper panel), Dateline (middle panel), and Spread (bottom panel) events.

Fig. 2. Idealized SSTa ($^{\circ}\text{C}$) for Eastern (upper panel), Dateline (middle panel), and Spread (bottom panel) events.

Fig. 3. Composite of precipitation anomalies (mm/day) of El Niño minus La Niña for a) Eastern, b) Dateline, and of Spread c) El Niño and d) La Niña events.

Fig. 4. Composite of 200mb eddy streamfunction anomalies ($10^6 m^2/s$) for a) Eastern El Niño minus La Niña b) Dateline El Niño minus La Niña, c) Spread El Niño and d) Spread La Niña events.

Fig. 5. Idealized experiments with ECHAM4 imposing positive SSTa. Upper panels are for Eastern, middle panels Dateline, and bottom panels Spread. Left column represents the eddy streamfunction ($10^6 m^2/s$) at 200mb, middle column the eddy streamfunction ($10^6 m^2/s$) at 850mb, while the right column represents precipitation anomalies (mm/day) and 850 mb winds (m/s).

Fig. 6. Idealized experiments with ECHAM4 using negative SSTa for Dateline (upper panels) and Spread (bottom panels). Left column is 200mb eddy streamfunction ($10^6 m^2/s$) and right column presents precipitation (mm/day) and 850m wind anomalies (m/s)

Fig. 7. Amip experiments with ECHAM4: Eddy streamfunction ($10^6 m^2/s$) at a) 200mb, b) 850mb, and c) precipitation anomalies and 850 mb anomalous winds (m/s) for Eastern El Niño. d) is the same as a) but for La Niña.

Fig. 8. Amip experiments with ECHAM4: Eddy streamfunction ($10^6 m^2/s$) at a) 200mb, b) 850mb, and c) precipitation anomalies for Dateline El Niño. d), e) and f) are the same as the upper panels but for Spread La Niña.

Fig. 9. Global observed precipitation anomalies (mm/day) for a) Eastern and b) Dateline).

Fig. 10. Composite of eddy streamfunction ($10^6 m^2/s$) anomalies of El Niño minus La Niña at a) 200mb and b) 850mb, as obtained with the ICTP AGCM

Fig. 11. Composites of observed eddy streamfunction ($10^6 m^2/s$) for Eastern El Niño minus La Niña at a) 400 mb and b) 850 mb. c) and d) are the same as a) and b) respectively but for Dateline.

Fig. 12. Composites of observed eddy streamfunction ($10^6 m^2/s$) for Spread El Niño at a) 850 mb, b) 400 mb, and c) 200 mb. Left panels are the same except for Spread La Niña.

598 **Figures**

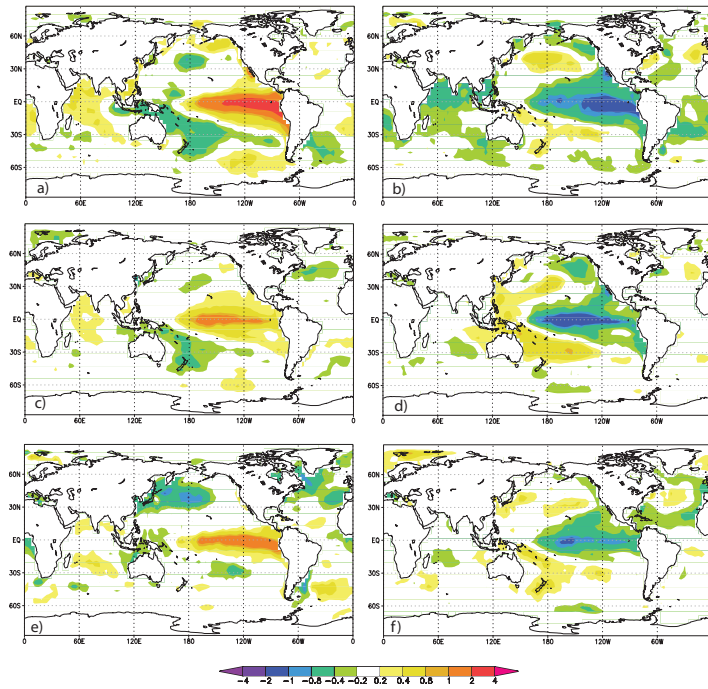


Fig. 1. Composite of observed SSTa ($^{\circ}$ C) for Eastern (upper panel), Dateline (middle panel), and Spread (bottom panel) events.

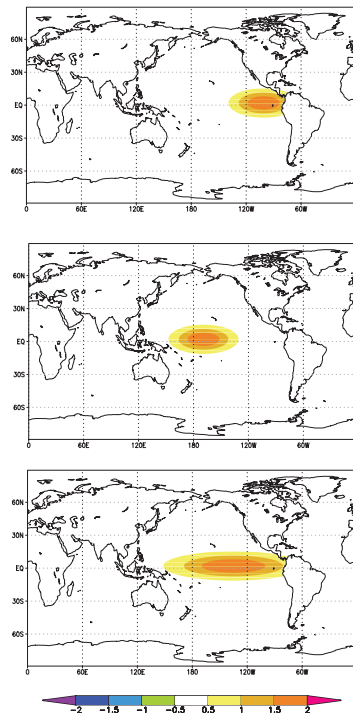


Fig. 2. Idealized SSTa ($^{\circ}\text{C}$) for Eastern (upper panel), Dateline (middle panel), and Spread (bottom panel) events.

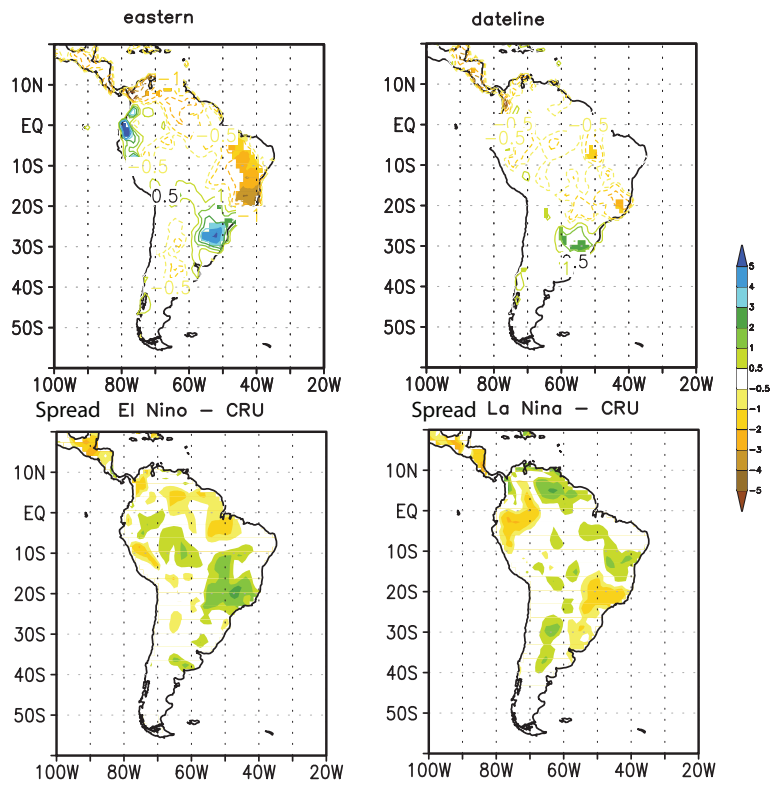


Fig. 3. Composite of precipitation anomalies (mm/day) of El Niño minus La Niña for a) Eastern, b) Date-line, and of Spread c) El Niño and d) La Niña events.

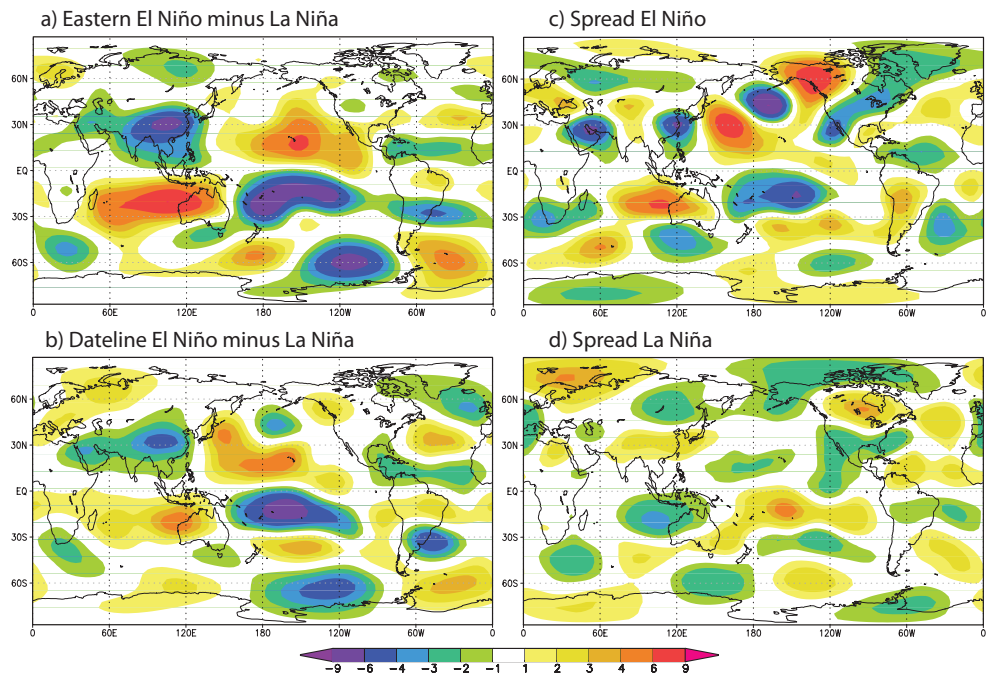


Fig. 4. Composite of 200mb eddy streamfunction anomalies ($10^6 m^2/s$) for a) Eastern El Niño minus La Niña b) Dateline El Niño minus La Niña, c) Spread El Niño and d) Spread La Niña events.

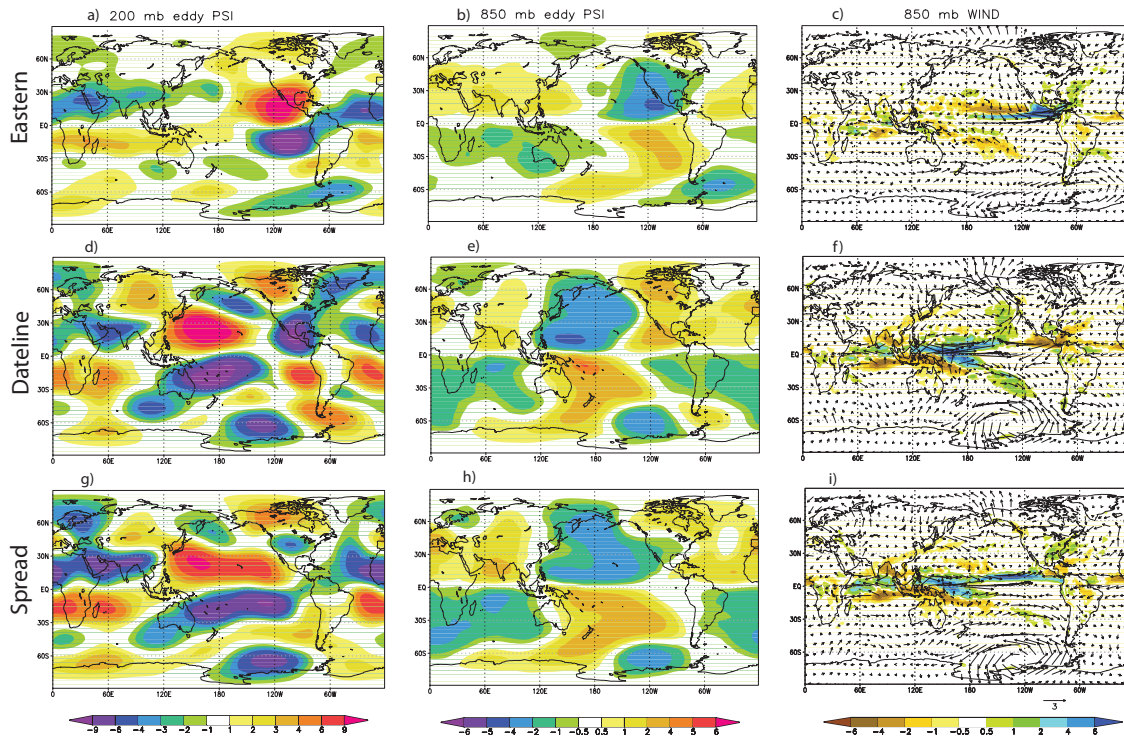


Fig. 5. Idealized experiments with ECHAM4 imposing positive SSTa. Upper panels are for Eastern, middle panels Dateline, and bottom panels Spread. Left column represents the eddy streamfunction ($10^6 m^2/s$) at 200mb, middle column the eddy streamfunction ($10^6 m^2/s$) at 850mb, while the right column represents precipitation anomalies (mm/day) and 850 mb winds (m/s).

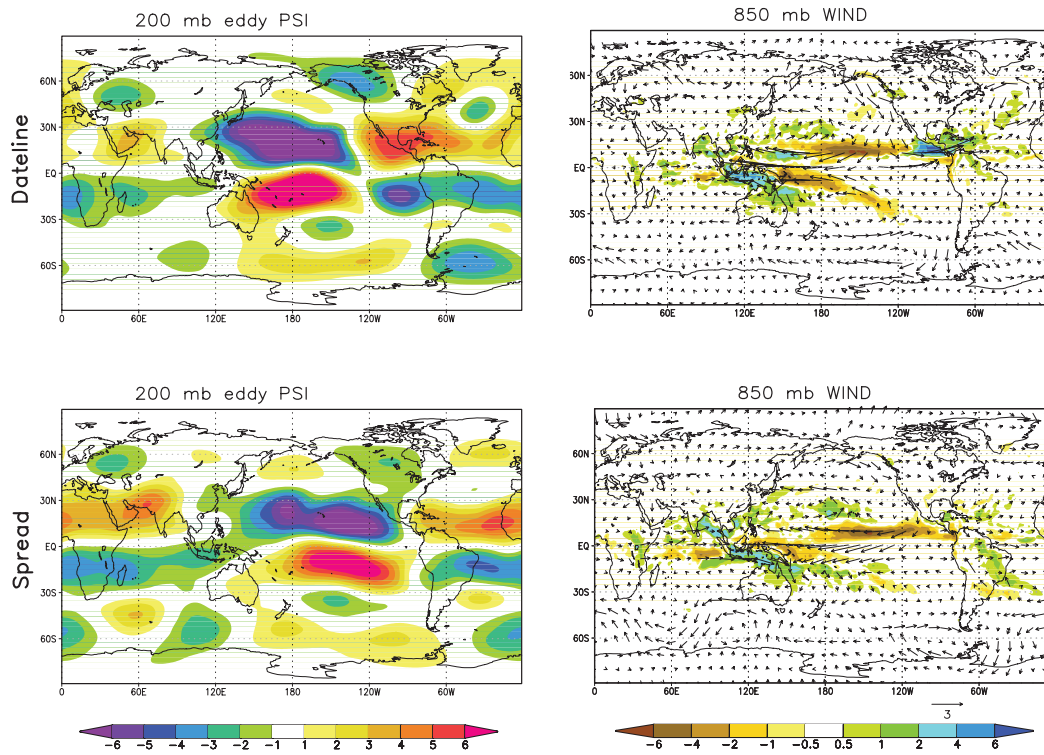


Fig. 6. Idealized experiments with ECHAM4 using negative SSTa for Dateline (upper panels) and Spread (bottom panels). Left column is 200mb eddy streamfunction ($10^6 m^2/s$) and right column presents precipitation (mm/day) and 850m wind anomalies (m/s)

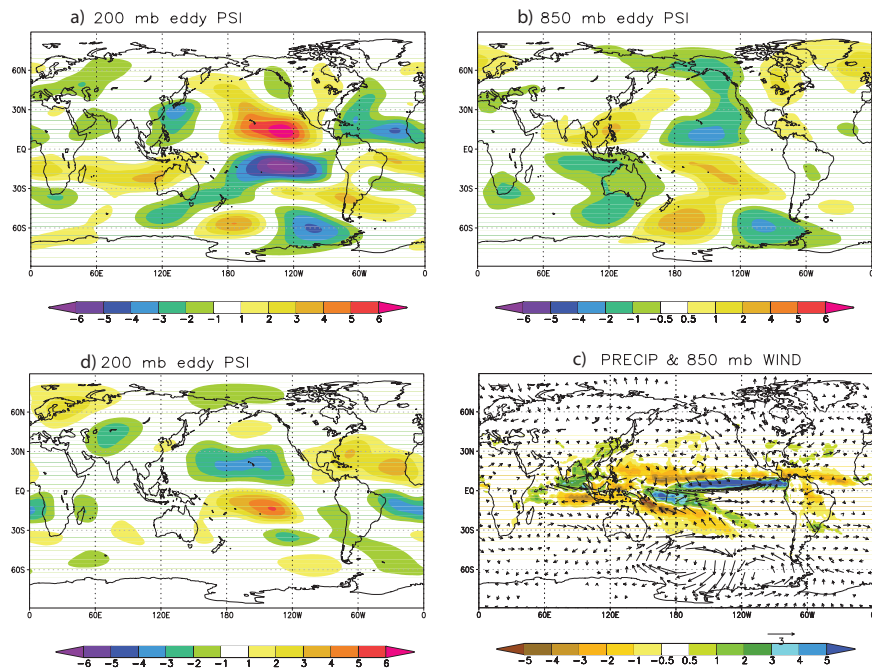


Fig. 7. Amip experiments with ECHAM4: Eddy streamfunction ($10^6 m^2/s$) at a) 200mb, b) 850mb, and c) precipitation anomalies and 850 mb anomalous winds (m/s) for Eastern El Niño. d) is the same as a) but for La Niña.

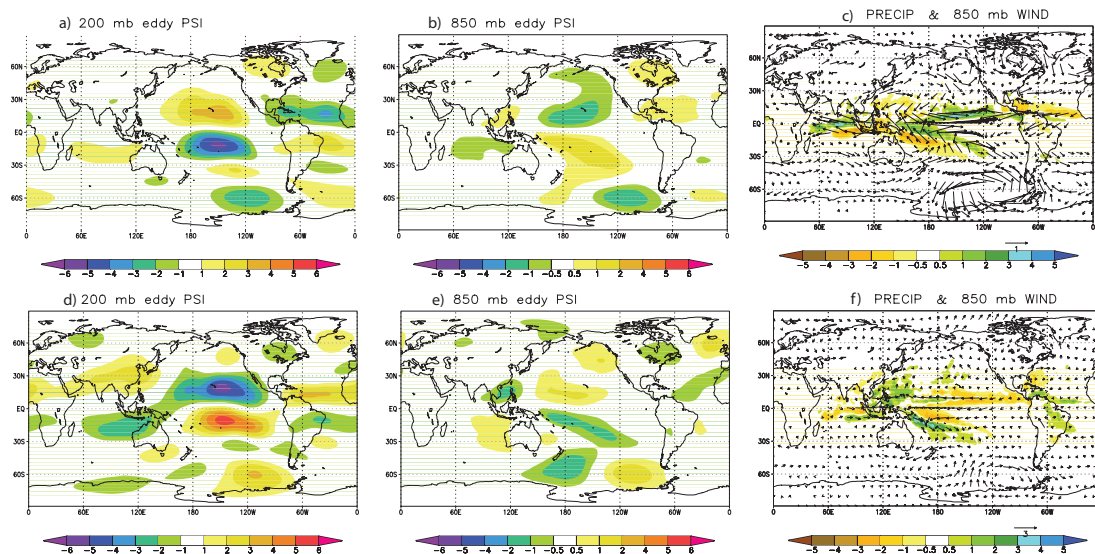


Fig. 8. Amip experiments with ECHAM4: Eddy streamfunction ($10^6 m^2/s$) at a) 200mb, b) 850mb, and c) precipitation anomalies for Dateline El Niño. d), e) and f) are the same as the upper panels but for Spread La Niña.

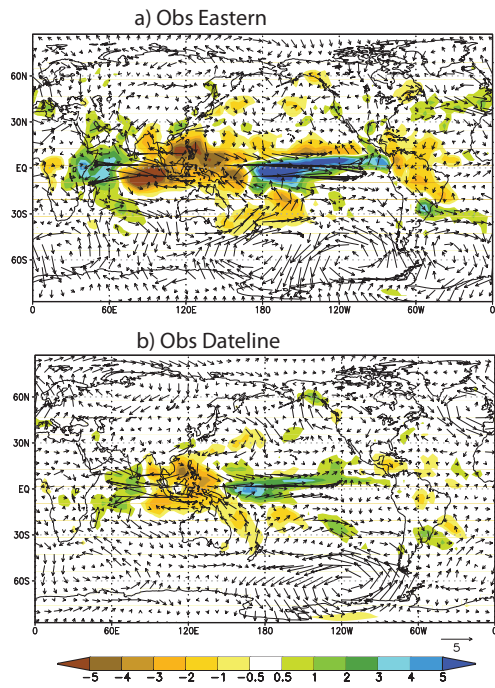


Fig. 9. Global observed precipitation anomalies (mm/day) for a) Eastern and b) Dateline).

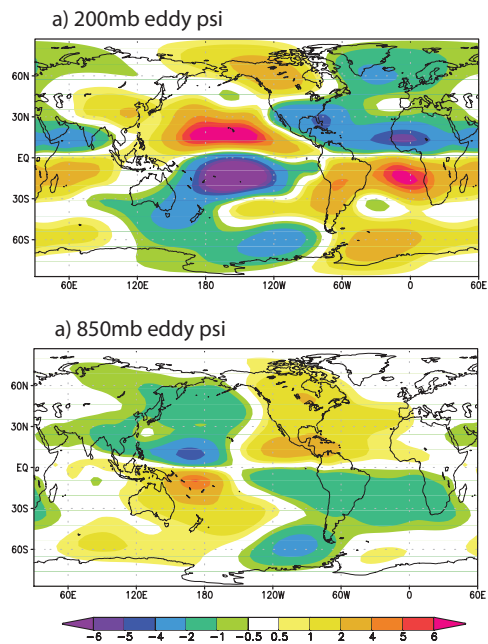


Fig. 10. Composite of eddy streamfunction ($10^6 m^2/s$) anomalies of El Niño minus La Niña at a) 200mb and b) 850mb, as obtained with the ICTP AGCM

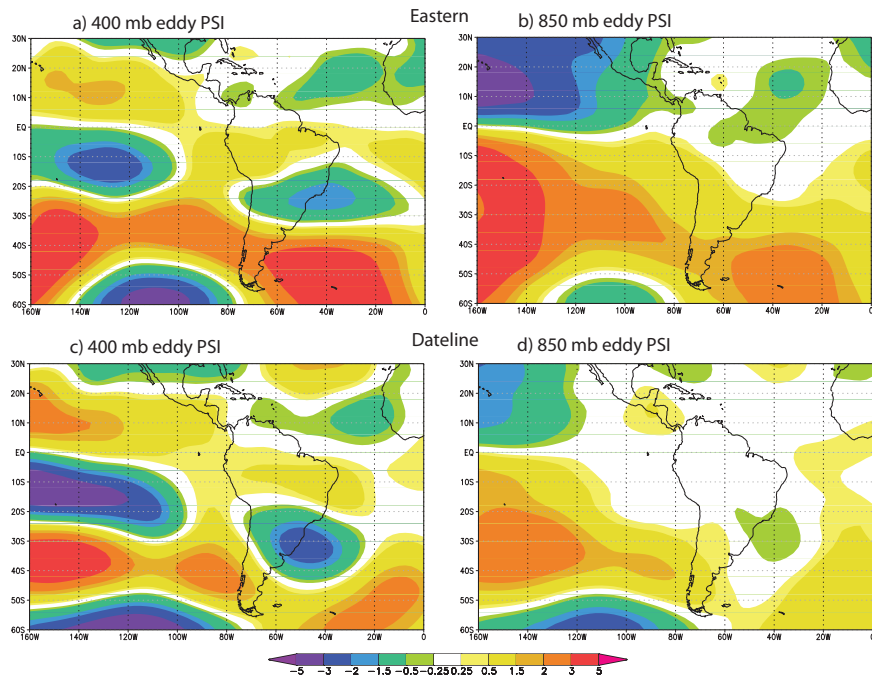


Fig. 11. Composites of observed eddy streamfunction ($10^6 m^2/s$) for Eastern El Niño minus La Niña at a) 400 mb and b) 850 mb. c) and d) are the same as a) and b) respectively but for Dateline.

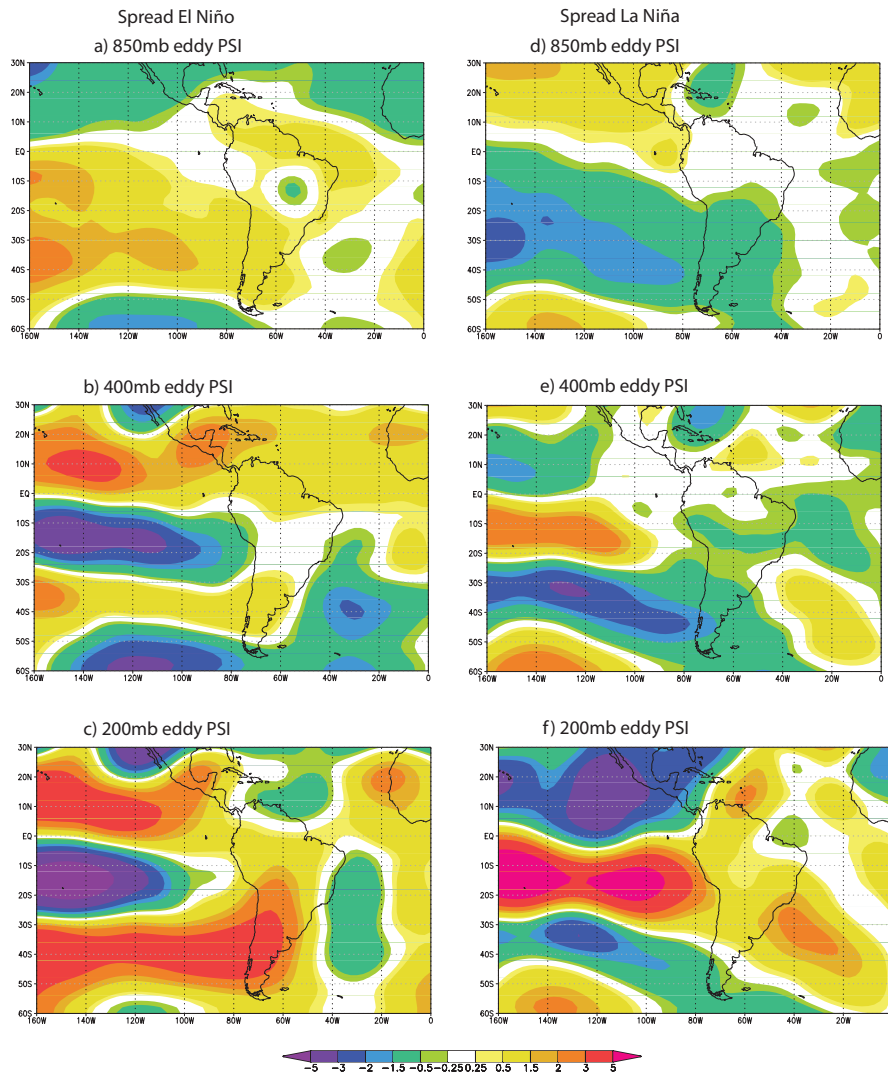


Fig. 12. Composites of observed eddy streamfunction ($10^6 m^2/s$) for Spread El Niño at a) 850 mb, b) 400 mb, and c) 200 mb. Left panels are the same except for Spread La Niña.